Int. J. Heat Mass Transfer. Vol. 30, No. 4, pp. 801–806, 1987
Printed in Great Britain

0017–9310/87 $3.00 + 0.00
Pergamon Journals Ltd.

A two-dimensional mathematical model of annular-dispersed and dispersed flows—II

P. L. KIRILLOV, V. M. KASHCHEYEV, Yu. V. MURANOV and Yu. S. YURIEV
Institute for Physics and Power Engineering, Obninsk, U.S.S.R.

(*Received* 4 *June* 1985)

Abstract—The results of computation by a two-dimensional mathematical model of a droplet-vapour flow are presented. The predicted two-phase flow characteristics, such as temperature, velocity and phase concentration fields, specific deposition flows, and the temperature of heat emitting surfaces are compared with experimental data. Some specific features of two-phase flow identified in calculations are analysed. The degree of the conservatism of some closing coefficients is numerically investigated. The calculations are performed over a wide range of operational parameters: $p = 0.147$–13.7 MPa, $\rho w = 260$–3000 kg m^{-2} s^{-1}.
The predicted results are found to be in reasonable agreement with the experimentally measured data.

1. THE NUMERICAL solution of the set of equations (23)–(69) presented in the first part of the paper [1] is considered as a computational experiment involving the verification of the model validity by comparing the measured and predicted data, comparison of calculated results with test problems, calculation of the parameters of specific steam generating channel operational modes, and numerical investigation of the specific features of a two-phase flow in the post-burnout region.

The computational experiment was conducted in the following sequence. The inlet flow parameters: pressure, mass flow rate, enthalpy, axial heat flux distribution are known, as well as the closing coefficients and functions given in the first part of the paper. Since the model describes two alternating flow modes—annular-dispersed and dispersed—then, having taken the reference point in the region of the annular-dispersed flow and specified the parameters in the initial cross-section, the lateral and axial characteristics of the system were calculated for the flow from the region of conventional heat removal (including the burnout cross-section) into the post-burnout region.

The model permits the evolution of local and integral flow characteristics throughout the channel to be followed. However, the possibilities of the computational experiment are not restricted to the calculation of characteristics realizable in each specific mode of vapour-generating channel operation. The influence of any parameter or a group of parameters involved in calculation within a wide range of their variation on the burnout heat transfer and heat transfer in the post-burnout region can be investigated numerically. Moreover, the computational experiment makes it possible to devise artificial situations, hardly created in physical rigs, when separate exchange effects are attenuated or augmented in the system to reveal the relationship between separate quantities in a 'pure' form.

Prior to calculations, the coefficient in the function of the distribution of mass sources in the diffusion equation, the wavenumber for the calculation of the coefficient taking account of droplet inertia, and the number of droplet groups were optimized and the method of dividing the ensemble of droplets into groups was developed.

2. The model allows the prediction of the following basic characteristics of annular-dispersed and dispersed flows: temperature, concentration and phase velocity fields; temperature of the heat emitting wall; local and integral deposition flows; cross-section-averaged liquid phase concentrations; liquid distribution in the core and the film; film thickness and velocity; mass flow rate in the film; heat transfer coefficients in the post-burnout region; mean vapour temperature; heat fractions in the post-burnout region lost by convection and by the evaporation of depositing droplets; decrease of the diameters of droplets moving in a superheated vapour.

The coolant characteristics were calculated for vertical, electrically heated tubes with a forced flow of a steam–water mixture and uniform and cosine axial heat flux distribution, typical of metal–water steam generators, within the following range of parameters: $p = 0.147$–13.7 MPa, $\rho w = 260$–2000 kg m^{-2} s^{-1}, $L = 1.5$–9 m, $d = 8$–12.7 mm, as well as for unheated tubes with $p = 2.9$–13.7 MPa, $\rho w = 500$–3000 kg m^{-2} s^{-1}, $L = 1.5$–3.66 m, $d = 8$–17 mm.

The reliability of the results obtained was checked by comparing the predicted results with the available experimental data. In Figs. 1–5 a comparison of some predicted and experimentally determined heat transfer characteristics of the flow is presented.

As an example of the prediction of some prescribed operational conditions for a steam-generating tube,

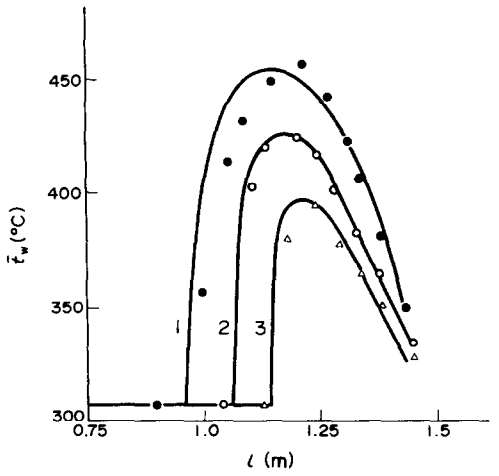

FIG. 1. The wall temperature in the case of cosine axial heat flux distribution: $p = 9.8$ MPa, $\rho w = 1500$ kg m^{-2} s^{-1}, $d = 10$ mm, $L = 1.5$ m, $x_{in} = 0.29$. 1, $Q = 27.3$ kW; 2, $Q = 25.8$ kW; 3, $Q = 24.7$ kW (——— calculation; ○ experimental data [2]).

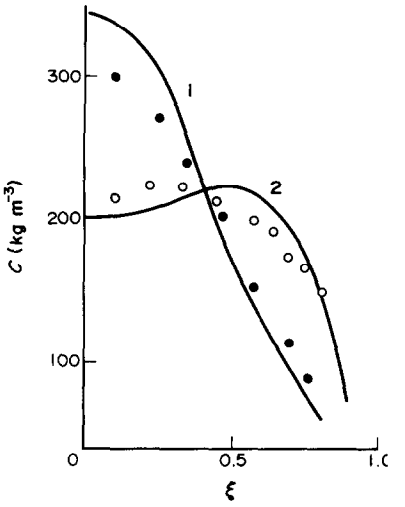

FIG. 3. Droplet concentration in the flow: $p = 13.7$ MPa, $\rho w = 750$ kg m^{-2} s^{-1}, $d = 17$ mm, $L = 3.6$ m. 1, $x = 0.3$; 2, $x = 0.2$ (——— calculation; ○ experimental data [4]).

Figs. 6–9 give the calculated flow parameters in the post-burnout zone of a single-tube model of a metal–water steam generator.

3. The computational experiment has revealed some specific features of post-burnout heat and mass transfer. When analysing the results obtained, it was discovered that the cross-sectional distribution of the concentration of the flow of droplets in dispersed flow in a heated channel is conservative with respect to the operational conditions. In all the calculations the maximum of the concentration curve is located in the central part of the flow (not necessarily along the axial line); in the wall region the droplet flow concentration smoothly decreases to zero at the wall.

Depending on the character of the droplet concentration distribution and the vapour temperature, two distinct drop-vapour flow patterns can be observed in the post-burnout region. The first pattern (Fig. 10) is characterized by the occurrence of two coexisting zones in the flow: the central zone, where the entire dispersed phase is concentrated and the vapour temperature is equal to the saturation temperature (region of thermal equilibrium); and the wall zone, where there are no droplets of liquid and the vapour is superheated. From the practical point of view, this mode is most unfavourable since it is characterized by maximum moisture ejection, high wall temperature and low heat transfer coefficients. Generally, the above mode of flow takes place at low mass velocities and high heat fluxes. The second, most common mode of dispersed flow, is characterized by superheating over the whole cross-section and by the

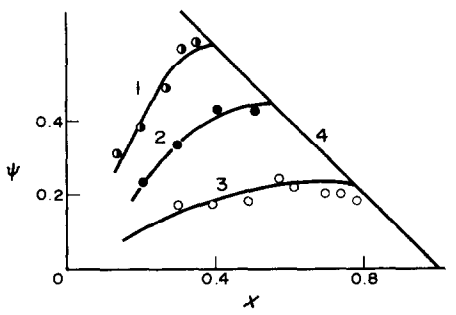

FIG. 2. Liquid fraction in the flow core: $p = 0.147$ MPa, $d = 8$ mm, $L = 2.5$ m. 1, $\rho w = 2000$ kg m^{-2} s^{-1}, $Q = 233$ kW; 2, $\rho w = 1000$ kg m^{-2} s^{-1}, $Q = 69$ kW; 3, $\rho w = 500$ kg m^{-2} s^{-1}, $Q = 50$ kW (——— calculation; ○ experimental data [3]).

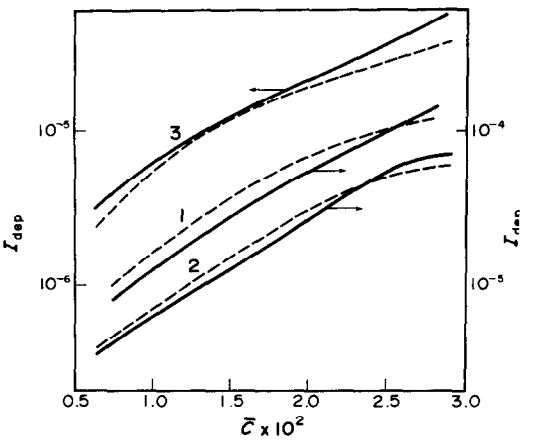

FIG. 4. Dimensionless specific drop deposition flow: $p = 6.9$ MPa, $x_{in} = 0.5$, $d = 13$ mm, $L = 2.5$ m. 1, $\rho w = 1000$ kg m^{-2} s^{-1}; 2, $\rho w = 2000$ kg m^{-2} s^{-1}; 3, $\rho w = 3000$ kg m^{-2} s^{-1} (– – – – calculation; ——— experimental data [5]).

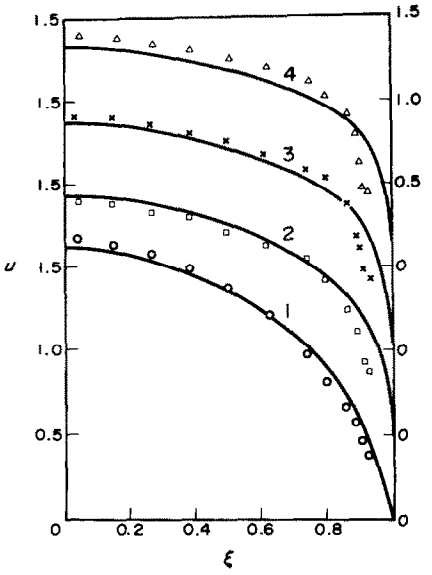

FIG. 5. Velocity profiles of vapour flow in a tube: 1, $x = 0.43$; 2, $x = 0.57$; 3, $x = 0.74$; 4, $x = 0.83$. $p = 6.9$ MPa, $\rho w = 500$ kg m^{-2} s^{-1}, $d = 17$ mm, $L = 3.6$ m (——— calculation; ○ experimental data [6]).

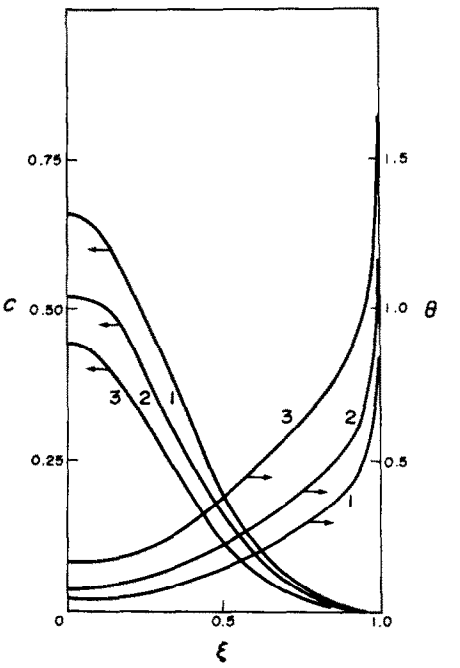

FIG. 7. Droplet flow concentration, C, and vapour temperature, θ, in the post-burnout zone: $p = 13.7$ MPa, $\rho w = 700$ kg m^{-2} s^{-1}, $Q = 123$ kW, $x_{in} = -0.48$, $d = 11$ mm, $L = 9$ m. 1, $\eta = 0.5$; 2, $\eta = 0.7$; 3, $\eta = 1.0$.

presence of liquid droplets at any point in the cross-section (Fig. 7).

The reason for the occurrence of the above flow patterns is due to the mechanical and thermal phase interactions in the flow. When the vapour superheating in the wall zone is significant and the droplets evaporating in it fail to reach the wall or when the vapour flow from the wall (for an annular-dispersed flow with film evaporation) prevents the droplets from depositing on the wall, one can speak of the thermal and mechanical screening of the deposition of droplets—it is in these conditions that the first, or separated, mode of droplet-vapour flow is developed.

It was also found from the analysis of predicted results that in a number of cases the deposition flow

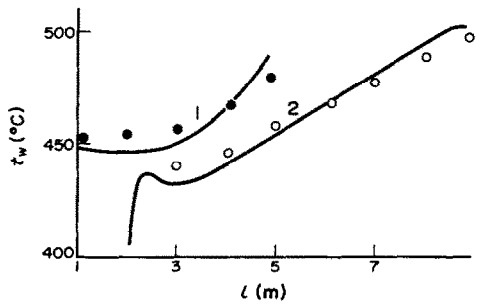

FIG. 6. The wall temperature in the post-burnout zone in a metal–water steam generator model. 1, $p = 15.7$ MPa, $\rho w = 350$ kg m^{-2} s^{-1}, $Q = 51$ kW, $x_{in} = -0.42$, $d = 11$ mm, $L = 5$ m; 2, $p = 13.7$ MPa, $\rho w = 700$ kg m^{-2} s^{-1}, $Q = 123$ kW, $x_{in} = -0.48$, $d = 11$ mm, $L = 9$ m (——— calculation; ○ experimental data [7]).

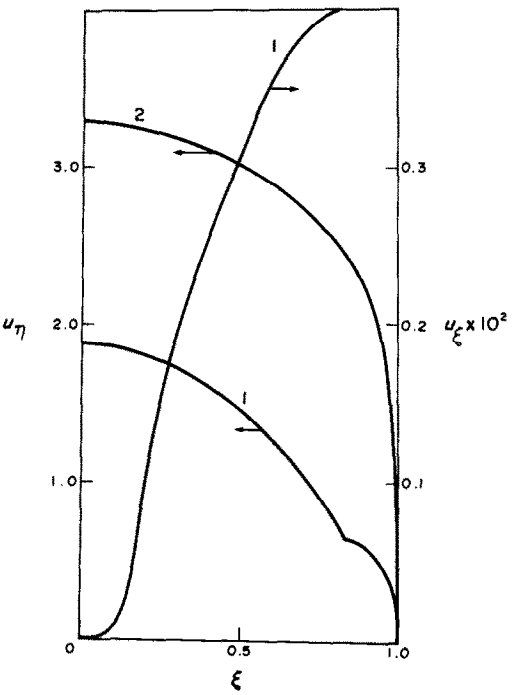

FIG. 8. The transversal, U_ξ, and longitudinal, U_η, velocity components of the vapour flow and the film velocity: $p = 13.7$ MPa, $\rho w = 700$ kg m^{-2} s^{-1}, $x_{in} = -0.48$, $d = 11$ mm, $L = 9$ m, $Q = 123$ kW. 1, $\eta = 0.2$; 2, $\eta = 0.7$.

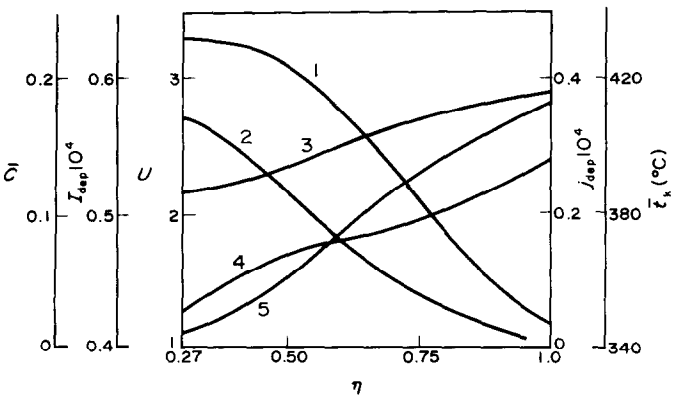

FIG. 9. Two-phase flow characteristics in the post-burnout region: $p = 13.7$ MPa, $\rho w = 700$ kg m^{-2} s^{-1}, $Q = 123$ kW, $x_{in} = -0.48$, $d = 11$ mm, $L = 9$ m. 1, J_{dep}; 2, $\bar{C}$; 3, $\bar{U}$; 4, t_w; 5, j_{dep}.

in the post-burnout region is a non-monotonous function of the channel length (Fig. 11). Two maxima are observed: in the burnout heat transfer region and in the region of transition to the unheated part of the channel. A non-monotonous character of the droplet deposition curve can also be attributed to a different intensity of the thermal and mechanical interaction of droplets with the vapour flow. Immediately after the burnout cross-section, the vapour flow from the wall due to liquid evaporation on it (there is no continuous film) is attenuated, as well as the vapour effect on the deposition of droplets, the wall layer is heated insufficiently and, as a consequence, an increase in the deposition flow is observed. The main reason for an increasing deposition flow in transition to the unheated part of the channel consists of a decreasing superheat in the wall region.

A distinctive feature of the zone of transition to the unheated part of the channel is the detected inversion of the temperature curves in the vapour flow (Fig. 12) caused by the fact that in the unheated part of the channel the droplets, being deposited on the wall, evaporate due to superheated vapour flow past the wetted wall; as a result, the temperature of the wall layer sharply decreases. It should be noted that the inversion of temperature curves in the droplet-vapour flow invariably takes place on the cessation of heat input.

4. In addition to studying the specific features of two-phase flow motion, the effect of inaccurate knowledge of some empirical relations used in the model was investigated, in particular, the effect of the distribution of the system parameters over the initial cross-section, the effect of the most probable size of a droplet in the droplet ensemble and of the entrainment

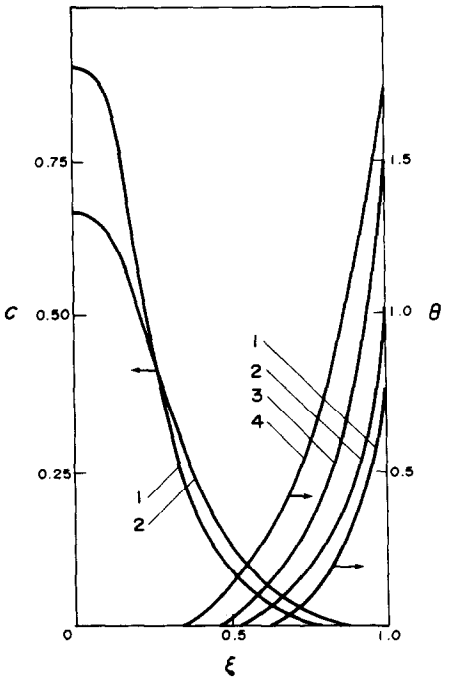

FIG. 10. Droplet flow concentration, C, and vapour temperature, θ, in the post-burnout zone: $p = 13.7$ MPa, $\rho w = 350$ kg m^{-2} s^{-1}, $Q = 41$ kW, $x_{in} = -0.08$, $d = 11$ mm, $L = 5$ m. 1, $\eta = 0.5$; 2, $\eta = 0.7$; 3, $\eta = 0.9$; 4, $\eta = 1$.

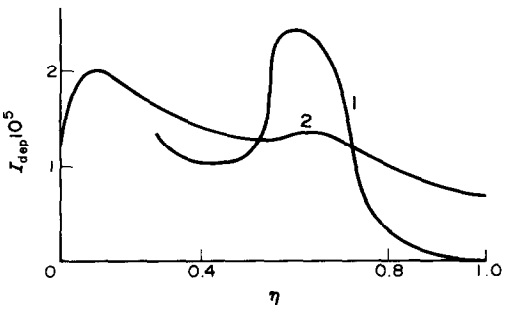

FIG. 11. Dimensionless specific deposition flow in the post-burnout zone: 1, $p = 9.8$ MPa, $\rho w = 260$ kg m^{-2} s^{-1}, $Q = 40.6$ kW, $x_{in} = -0.09$, $d = 11$ mm, $L = 13$ m; 2, $p = 13.7$ MPa, $\rho w = 260$ kg m^{-2} s^{-1}, $Q = 37.3$ kW, $x_{in} = -0.24$, $d = 11$ mm, $L = 13$ m.

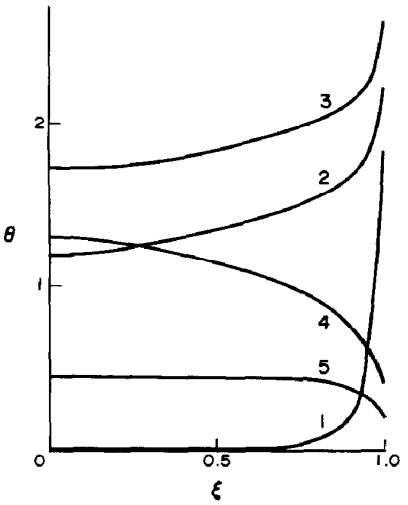

FIG. 12. Vapour temperature in the post-burnout and adiabatic regions: $p = 13.7$ MPa, $\rho w = 260\ \mathrm{kg\,m^{-2}\,s^{-1}}$, $Q = 37.3$ kW, $x_{in} = -0.24$, $d = 11$ mm, $L = 13$ m. 1, $\eta = 0.1$; 2, $\eta = 0.3$; 3, $\eta = 0.5$; 4, $\eta = 0.7$; 5, $\eta = 0.8$.

flow and the effect of the technique of droplet ensemble division into groups and of the number of droplet groups.

When selecting the coordinate for the reference point, the distribution of liquid between the core and the film was prescribed, as well as the function of the droplet flow concentration distribution over the cross-section. Of course, the above characteristics were prescribed quite approximately. The degree of the effect of this approximation was investigated by varying the initial coordinate. An inaccurate assignment of parameters over the initial cross-section was found to be largely compensated for by the mechanism incorporated into the model by removing the reference point from the region or the cross-section under consideration. In general, the reference point can be selected in any cross-section along the length of the channel where there is an annular dispersed flow and this possibility is admitted in the initial expressions, however, it is desirable that the calculation be started in the zone most removed from the cross-section investigated.

The effect of the mean diameter in the droplet ensemble was investigated because of the expansion of the empirical formula validity range in the calculations made [1]. The calculations have shown that the effect of the most probable droplet size on the results obtained increases with a decrease of the droplet diameter. For highly dispersed systems, the departure of the most probable droplet size from the real one shows up most appreciably in calculations.

Also, the influence of the entrainment flow on the coordinate of the burnout heat transfer section and some characteristics of the post-burnout zone were investigated. The entrainment flow is calculated by the empirical relation of ref. [1] within ±20%. It is shown that in fixed operational conditions an artificial variation of the entrainment flow results in appropriate changes in the deposition flow, and for small mass flow rates of a steam–water mixture, the entrainment and deposition flows compensate each other to a great extent. Then, the evaporation flow starts to play a considerable role in the development of thermal crises. The dynamics of the system is such that it leads to a partial levelling of the effect of transversal mass fluxes on the parameters at the burnout heat transfer section. This factor characterizes the entrainment flow as a conservative quantity.

As noted above, to this type of investigation belong the experiments on the determination of the number of droplet groups and the technique for droplet ensemble division into groups. The calculations have shown that the use of the monodisperse approximation alone may lead to the departure of such calculated quantities as the coordinate of the burnout heat transfer section and the relative temperature of the heat emitting wall from the appropriate experimental data by 30% and more. It is found that the number of groups giving a satisfactory agreement between the measured and predicted quantities is between five and six. A further increase in the number of groups gives a slight decrease of the discrepancy between the experimental and predicted quantities. The analysis has shown that the most effective techniques for the division of the droplet ensemble into groups is that which is based on the equality of weight fractions for each group. This technique allows the effect of each group on mass transfer processes to be properly taken into account.

5. Thus, the use of all the conservation laws presented in terms of partial two-dimensional equations enables a considerable body of information on annular-dispersed and dispersed flows to be obtained. Since the closing of the equations was performed on the differential level, the closing coefficients and functions are generally conservative with respect to the results obtained. There are no freely varying numerical factors which would have corrected the range of validity of the model. In all probability, a further improvement of the model should be connected with taking account of the unsteady-state character of the phenomena, development of the physical picture and mathematical description of the entrainment phenomena, with the transformation of the model itself to extend it to complex channels.

REFERENCES

1. P. L. Kirillov, V. M. Kashcheyev, Yu. V. Muranov and Yu. S. Yuriev, A two-dimensional mathematical model of annular-dispersed and dispersed flows—I, *Int. J. Heat Mass Transfer* **30**, 791–800 (1987).
2. O. V. Remizov, V. A. Vorobiyov and N. G. Shurkin, Burnout and the dynamics of its development in a tube with a cosine-law heat release along the length with forced flow of water, Preprint of the Institute for Physics and Power Engineering, No. 481, Obninsk (1974).

3. S. P. Kaznovsky, R. S. Pometko and V. V. Pashichev, The burnout and liquid distribution in annular dispersed mode of flow, *Teplofiz. Vysok. Temp.* **16,** 94–100 (1978).
4. P. L. Kirillov, I. P. Smogalev and M. Ya. Suvorov, Liquid distribution in an annular dispersed steam–water high-pressure flow, Preprint of the Institute for Physics and Power Engineering, No. 810, Obninsk (1978).
5. B. I. Nigmatulin, V. I. Milashenko and V. E. Nikolayev, Experimental investigation of the hydrodynamics of equilibrium annular dispersed steam–water flows, *Teplofiz. Vysok. Temp.* **16,** 1281–1286 (1978).
6. P. L. Kirillov, N. M. Komarov and V. I. Subbotin, Measurement of certain vapour–liquid flow characteristics in a circular tube at a pressure of 6.9 MPa, Preprint of the Institute for Physics and Power Engineering, No. 421, Obninsk (1973).
7. N. S. Grachyov, V. M. Kashcheyev and Yu. V. Muranov, Calculation of heat and mass transfer characteristics in the post dryout zone of 'sodium–water' vapour generator, Preprint of the Institute for Physics and Power Engineering, No. 885, Obninsk (1978).

UN MODELE MATHEMATIQUE BIDIMENSIONNEL DES ECOULEMENTS DISPERSES ANNULAIRES ET DISPERSES—II

Résumé—On présente les résultats de calcul par un modèle mathématique bidimensionnel, de l'écoulement vapeur-gouttes. On compare avec les données expérimentales les caractéristiques calculées de l'écoulement diphasique telles que les champs de température, de vitesse et de concentration de phase et la température de la surface chaude émettrice. Quelques résultats spécifiques de l'écoulement diphasique identifiés dans les calculs sont analysés. Le degré de conservatisme de quelques coefficients de fermeture sont étudiés numériquement. Les calculs sont effectués pour un large domaine de paramètres opérationnels: $p = 0{,}147$–$13{,}7$ MPa, $\rho w = 260$–3000 kg m^{-2} s^{-1}. Les résultats du calcul sont trouvés être en accord raisonnable avec les données expérimentales.

EIN ZWEIDIMENSIONALES MATHEMATISCHES MODELL FÜR DEN ÜBERGANGSBEREICH RING-/SPRÜHSTRÖMUNG SOWIE FÜR SPRÜHSTRÖMUNG, TEIL II

Zusammenfassung—Ergebnisse der Berechnungen eines zweidimensionalen mathematischen Modells einer Dampf/Tropfenströmung werden vorgelegt. Die berechneten Charakteristiken der Zweiphasenströmung wie die Verteilungen von Temperatur, Geschwindigkeit und Phasenkonzentration, spezielle Niederschlagsströmungen und die Temperaturen der wärmeabgebenden Oberflächen werden mit experimentellen Daten verglichen. Einige spezielle Gesichtspunkte der Zweiphasenströmung, die in den Berechnungen festgestellt wurden, werden analysiert. Der Grad des Konservatismus einiger Schließungs-Koeffizienten wird numerisch untersucht. Die Berechnungen werden über einen weiten Bereich von Betriebsparametern durchgeführt: $p = 0{,}147$–$13{,}7$ MPa, $\rho_w = 260$–3000 kg m^{-2} s^{-1}. Die Ergebnisse der Berechnungen stimmen gut mit den experimentellen Meßdaten überein.

ДВУМЕРНАЯ МАТЕМАТИЧЕСКАЯ МОДЕЛЬ ДИСПЕРСНО-КОЛЬЦЕВОГО И ДИСПЕРСНОГО ПОТОКОВ — II

Аннотация—Представлены результаты вычислительного эксперимента по двумерной математической модели парокапельного потока. Расчетные характеристики двухфазного потока (поля температур, скоростей и концентраций фаз, удельные потоки орошения, температура теплоотдающей поверхности) представлены в сравнении с опытными данными. Проанализированы некоторые особенности в движении двухфазного потока, установленные при проведении расчетов. Численно исследована степень консервативности некоторых замыкающих коэффициентов. Расчеты проведены в широком диапазоне режимных параметров $P = 0{,}147$–$15{,}7$ МПа, $\rho_w =$ (260–3000) кг м$^{-2}$ с$^{-1}$. Наблюдается удовлетворительное совпадение расчетных и опытных величин.